VIII Workshop-Escola de Computação e Informação Quântica & VIII Workshop de Computação Quântica - UFSC, 08–12 de Dezembro de 2025, Florianópolis, SC

Hong-Ou-Mandel Interference in Multicore Fibers: Measurements at Subpicosecond Precision

Letícia Tacca[1], Lucas Fagundes[2], Gustavo Santos[1], Gustavo Lima[1], Esteban Gómez[1], Stephen Walborn[1]

Abstract— **The Hong-Ou-Mandel (HOM) effect, key to quantum interference, is well known in two-port systems but less explored in multiport photonic circuits. We experimentally demonstrate HOM interference across multiple outputs using fiber-integrated photonic platforms, revealing new bunching and anti-bunching regimes. As an application, we measure the intercore differential mode delay in multicore fibers with subpicosecond precision. Our setup, combining superconducting detectors and tunable delay lines, maps multiport interference and matches theoretical models. These results open paths for quantum-enhanced metrology, communications, and multi-channel quantum gates, advancing both the understanding and practical use of quantum interference in complex integrated photonic systems.**

Keywords— **Quantum interference, Hong-Ou-Mandel effect, multicore fibers, photon bunching/anti-bunching, quantum-enhanced measurements.**

I. Introduction

Quantum interference lies at the core of many quantum technologies, from secure communication protocols to sensing [1, 2]. It occurs when distinct quantum mechanical outcomes are indistinguishable. If two photons enter a symmetric 2×2 beamsplitter (one photon per input), the trajectories for *both photons reflecting* versus *both transmitting* are fundamentally indistinguishable. This triggers destructive interference, forcing the photons to always exit together in a superposition state — never separately.

Classically, particles would separate 50% of the time. Scanning photon arrival times reveals a Hong-Ou-Mandel (HOM) [3] dip: coincidence rates plunge to near zero at zero delay (full quantum interference) but rise to the classical 50% baseline at finite delays. The dip's width reflects photon coherence time, while its visibility V (depth, $0 \leq V \leq 1$) quantifies interference quality. Any distinguishing information (e.g., polarization, frequency mismatches) degrades $V < 1$.

In this work, after detailing our 4×4 multicore fiber (MCF) device and setup, we investigate multiport HOM interference in fiber-integrated photonic circuits, observing non-classical photon correlations across multiple outputs. This approach extends traditional two-photon interference into higher dimensions, enabling new capabilities in quantum metrology. As a key application, we demonstrate subpicosecond precision in measuring intercore delays in multicore fibers - a promising tool for quantum-enhanced synchronization and sensing.

[1] Departamento de Física, Universidad de Concepción, Concepción, Chile, e-mail: letacca@udec.cl;
[2] Universidade Federal de Santa Catarina, Florianópolis.SC, Brasil.

II. Model of HOM interference with 4×4 MCF beam splitter

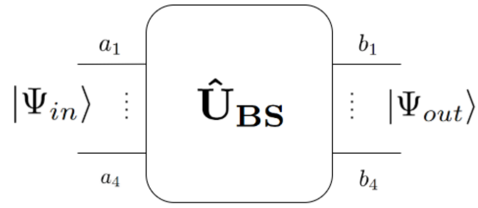

Fig. 1. Action of a 4x4 multiport BS on a quantum state.

In a 4×4 HOM interference experiment, the transformation of input photon modes through a symmetric 4-port beam splitter is described by a unitary matrix U, typically chosen as the 4-dimensional unitary matrix [4]:

$$U = \frac{1}{2}\begin{bmatrix} 1 & 1 & 1 & 1 \\ 1 & i & -1 & -i \\ 1 & -1 & 1 & -1 \\ 1 & -i & -1 & i \end{bmatrix} \tag{1}$$

Each input creation operator $\hat{a}_j^\dagger$ transforms into an output mode $\hat{b}_k^\dagger$ according to:

$$\hat{b}_k^\dagger = \sum_{j=1}^{4} U_{kj}\hat{a}_j^\dagger \tag{2}$$

If two indistinguishable photons are injected into input modes i and j, the output state is given by:

$$|\psi_{\text{out}}\rangle = \sum_{k,l=1}^{4} U_{ki}U_{lj}\,\hat{b}_k^\dagger\hat{b}_l^\dagger\,|0\rangle \tag{3}$$

Due to bosonic symmetry, the interference of indistinguishable photons leads to **non-classical correlations** in the output. In particular, **bunching** and **anti-bunching** effects.

The plot in Fig. 2 shows the theoretical coincidence probabilities for two indistinguishable photons passing through a 4×4 beam splitter, exhibiting characteristic bunching (dips) and anti-bunching (peaks) behavior. The coincidence probability between output ports i and j depends on the interference of indistinguishable paths and can be expressed as

$$P_{ij}(\tau) \propto \left|U_{i1}U_{j2} + e^{i\phi(\tau)}U_{j1}U_{i2}\right|^2, \tag{4}$$

where $\phi(\tau)$ is the relative phase depending on the temporal delay τ between photons. For certain output pairs, the interference is destructive, leading to reduced coincidence counts

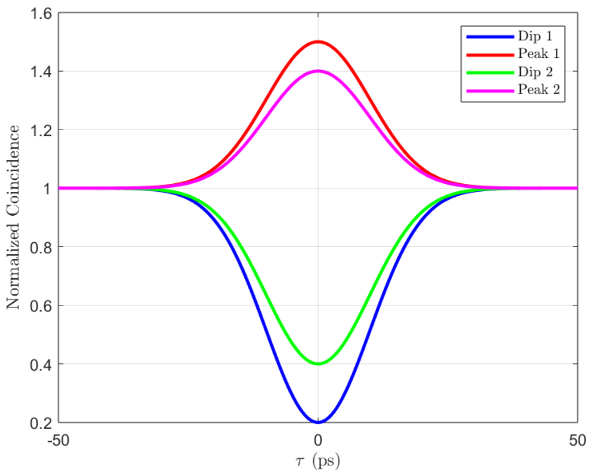

Fig. 2. Model for the HOM dips (bunching) and peaks (anti-bunching) in a 4x4 multiport BS.

(bunching dips), while for others it is constructive, resulting in enhanced coincidence counts (anti-bunching peaks). The Gaussian envelope in the plot models the temporal overlap of the photon wave packets, which governs the visibility of these interference effects.

III. Intercore Differential Group Delay (IDGD) and Mode Dispersion

Intercore Differential Group Delay (IDGD), or also called *mode delay*, is a critical parameter in MCF systems, representing the temporal delay difference between signals propagating through different cores in a medium of length L. It originates from core-to-core variations in group velocity, which may stem from minor structural or refractive index differences, stress-induced birefringence, or environmental perturbations such as bending and temperature changes [5].

Mathematically, the IDGD between cores i and j over a fiber of length L is expressed as:

$$\Delta\tau_{ij} = L \cdot \left(\frac{1}{v_{gi}} - \frac{1}{v_{gj}} \right) = \frac{L}{c} \cdot (n_{gi} - n_{gj}) \,, \qquad (5)$$

where $\Delta\tau_{ij}$ is the differential group delay (in seconds), v_{gi}, v_{gj} are the group velocities in cores i and j, n_{gi}, n_{gj} are the group refractive indices, L is the fiber length, and c is the speed of light in vacuum.

If IDGD depends only on a constant difference in the refractive indexes of each core, then we would expect it to grow linearly with L. This was the premise behind the proposed scheme in Ref. [6], in which they found that another type of behavior dominated. On the other hand, if IDGD is due to random imperfections along the fiber length (not a constant difference in index of refraction, but rather positive and negative differences that vary along the fiber length, like a random walk), we expect

$$IDGD = \Delta \times \sqrt{L}, \qquad (6)$$

where Δ is the mode dispersion, in units of $time/\sqrt{distance}$ or equivalent. Note that polarization mode dispersion (PMD) follows a relation like this [5].

This work aims to use HOM interference to investigate whether IDGD behavior follows this random walk-like relation for the first time.

IV. Methodology

A. Experimental setup

We measured quantum interference in MCF devices using photon pairs generated via spontaneous parametric down-conversion (SPDC), as shown in Fig. 3. A type-II periodically poled potassium titanyl phosphate (PPKTP) crystal, pumped by a 65 mW pulsed laser at 775 nm, produced photon pairs at 1550 nm. These photons passed through a 30 nm interference filter (IF) before being coupled into single-mode fibers (SMFs). The photons were then routed through a modified Mach-Zehnder interferometer (MZI), starting with a polarizing beamsplitter (PBS) that separated them by polarization. The output was directed to the MCF system (see Fig. 4), comprising fiber-optic demultiplexers and an MCF beamsplitter (MCF-BS). After interference in the MCF-BS, single photons were detected by superconducting nanowire single-photon detectors (SNSPDs), with coincidences registered using a field-programmable gate array (FPGA) system.

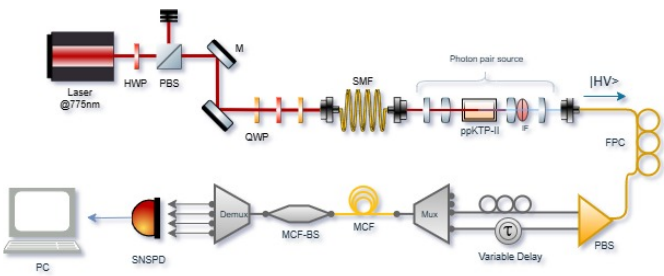

Fig. 3. Experimental setup for HOM interference using multicore fibers.

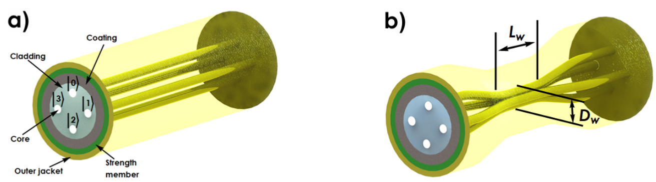

(a) Multicore fiber with 4 cores.

(b) MCF beam splitter.

Fig. 4. MCF technology.

B. How to measure IDGD with HOM interferometer

The HOM interferometer can be used to measure the delay time between two paths as in Fig. 5. If each path is a different "mode", then the HOM measures IDGD directly.

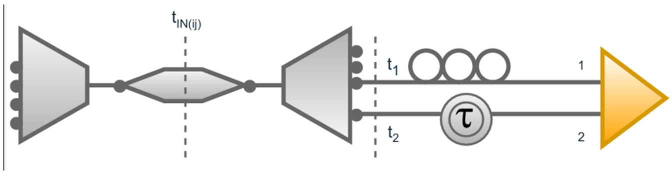

Fig. 5. Mach-Zender interferometer showing the flight time of the photons after the PBS (yellow triangle) until the MCF-BS ($t_{IN(ij)}$).

$$\text{HOM}_{ij} = t_1 + t_i - (t_2 + t_j)$$
$$\text{HOM}_{ji} = t_1 + t_j - (t_2 + t_i)$$

$$\Delta \rightarrow \text{HOM}_{ij} - \text{HOM}_{ji} = 2(t_i - t_j) \tag{7}$$

The above equation relates the IDGD to the difference in the dip positions of the HOM without the length L of the MCF, which we call the "control". It works as a reference starting point. When we add MCFs between the first DEMUX and the MCF-BS, we repeat the HOM measurements. Then, for the final calculation and plot for the IDGDs, we need to rest the control delays for each combinations of cores (see Fig. 8).

C. Measurement and Statistical Analysis

We measured IDGD for all twelve combinations fiber cores, obtaining a set of six values for a given fiber length L: $\{\text{IDGD}_1, \text{IDGD}_2, \ldots \text{IDGD}_6\}$. The DGD values are positive, random numbers — not symmetrically distributed around a mean (at least in the case of few measurements). Thus we compute the root mean square (RMS) of the IDGD values: $IDGD_{RMS} = \sqrt{\langle(\text{IDGD})^2\rangle}$. Then,

$$IDGD_{RMS} = \Delta \times \sqrt{L} + c, \tag{8}$$

where c is the constant delay due to the SMF fiber inputs.

V. Results and Analysis

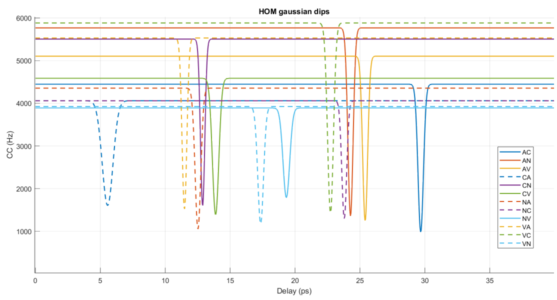

Fig. 6. HOM curves for the MZI interferometer (control case, considering the accidental coincidences). Each core in the MCF is labeled by a letter: A, C, N, and V (for the colors names in spanish: Azul, Café, Naranja, Verde). Then, each pair represents a coincidence count rate for different combinations of the first DEMUX input. IDGD values are extracted from this plot, that gives directly the delays of distint core combinations.

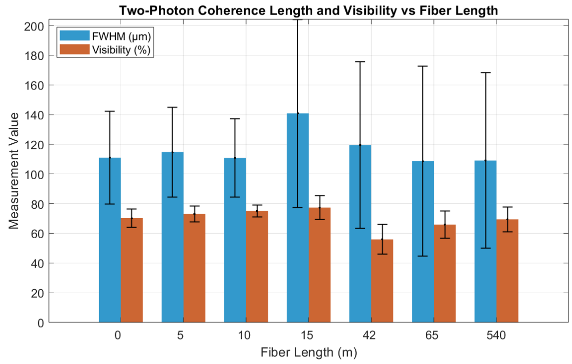

Fig. 7. Two-photon interference metrics vs. fiber length. Blue bars represent the coherence length (L_o, left axis), derived from the HOM dip FWHM via $L_o = c\tau_o/n$, where τ_o is the coherence time and $n = 1.444$ the fiber refractive index. Orange bars: Interference visibility (right axis, %). Error bars represent ±1 standard deviation across measurements.

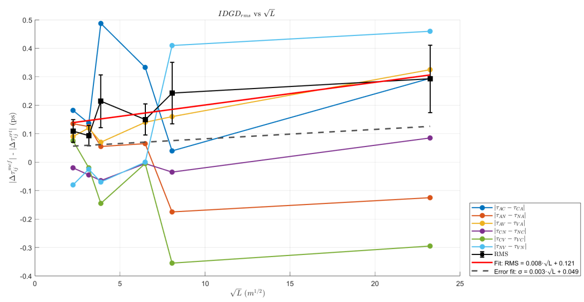

Fig. 8. Root mean square of IDGD values and linear fit.

The RMS of IDGD between cores increases proportionally to the square root of the fiber length (RMS $\propto \sqrt{L}$), in agreement with theoretical predictions for randomly coupled cores. The fitted model displayed good consistency with the experimental data, supporting the assumption of stochastic DGD accumulation. The extracted coefficient Δ (in units of ps $\cdot$ m$^{-1/2}$) serves as a characteristic measure of the average differential mode dispersion per $\sqrt{\text{m}}$. Moreover, when considering the dispersion per $\sqrt{\text{km}}$, the value obtained in the RMS fit is $\Delta = 0.008$ ps$/\sqrt{\text{m}} = 0.253$ ps$/\sqrt{\text{km}}$. This Δ value is in the typical PMD coefficient range ($0.1 \leq \sigma_{\text{PMD}} \leq 1$ ps$/\sqrt{\text{km}}$), what could indicate some polarization dispersion effect. However, more careful analysis is required to confirm this interpretation since HOM interference may yield distinct dispersion characteristics compared to conventional PMD measurements.

VI. Conclusion

We demonstrated multiport Hong-Ou-Mandel interference in a 4×4 multicore fiber beam splitter, observing non-classical photon correlations across multiple outputs. Applying this to intercore differential group delay (IDGD) measurements, we found the root mean square of IDGD scales as $\sqrt{L}$ ($\Delta = 0.253$ ps$/\sqrt{\text{km}}$), consistent with stochastic mode dispersion. While this Δ value falls within typical polarization mode dispersion ranges, we note that HOM interference probes dispersion through phase-insensitive two-photon correlations rather than single-mode phase delays. This distinction, coupled with the polarization-sensitive nature of quantum interference, suggests IDGD may reflect unique physical mechanisms warranting further investigation. This work establishes quantum interference as a powerful tool for precision metrology in complex photonic systems.

Acknowledgments

We thank the Fondo Nacional de Desarrollo Científico y Tecnológico (ANID) (Grants 1200266, 1240746), ANID – Millennium Science Initiative Program – ICN17_012 and project UCO 1866.

References

[1] ZL Yuan et al. “Interference of short optical pulses from independent gain-switched laser diodes for quantum secure communications”. In: *Physical Review Applied* 2.6 (2014), p. 064006.

[2] Henry Semenenko et al. “Interference between independent photonic integrated devices for quantum key distribution”. In: *Optics letters* 44.2 (2019), pp. 275–278.

[3] Chong-Ki Hong, Zhe-Yu Ou, and Leonard Mandel. “Measurement of subpicosecond time intervals between two photons by interference”. In: *Physical review letters* 59.18 (1987), p. 2044.

[4] J Cariñe et al. “Multi-core fiber integrated multi-port beam splitters for quantum information processing”. In: *Optica* 7.5 (2020), pp. 542–550.

[5] Bahaa EA Saleh and Malvin Carl Teich. *Fundamentals of photonics, 2 volume set*. john Wiley & sons, 2019.

[6] Hee Jung Lee, Eunjoo Lee, and Hee Su Park. “Azimuth-Rotated Splicings of a Four-Core Optical Fiber for Inter-Core Group Delay Compensation”. In: *IEEE Photonics Technology Letters* 29.24 (2017), pp. 2250–2253. DOI: 10.1109/LPT.2017.2771248.